RSC Advances

ROYAL SOCIETY
OF **CHEMISTRY**

www.rsc.org/advances

Novel Ag-ZnO nanostructured Brushes

RSC Advances
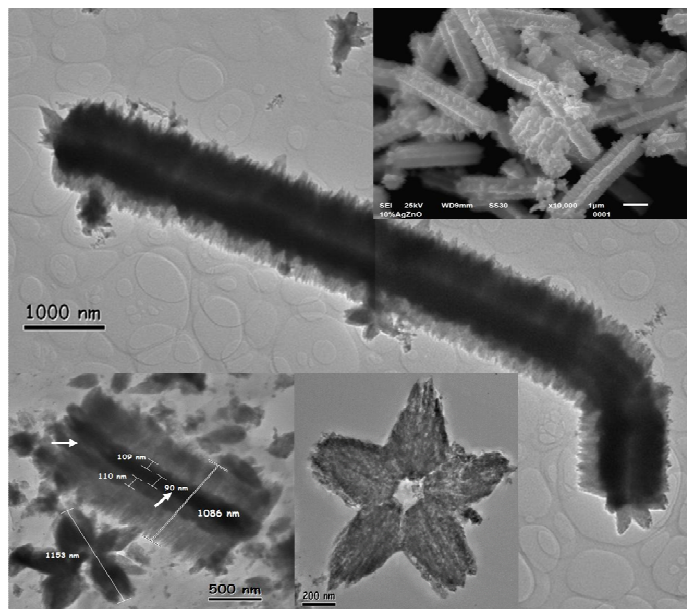
ARTICLE

Ag nanowires as precursors to synthesize Ag-ZnO nanostructured Brushes

Gilberto Mondragón-Galicia, Claudia Gutiérrez-Wing, Ma. Eufemia Fernández-García, Demetrio Mendoza-Anaya, Raúl Pérez-Hernández*

Abstract Ag-ZnO nanostructured brushes (NBs) were synthesized by the precipitation method. From this study, it was evidenced that a key parameter to grow these unidirectional structures is the seeding through Ag nanowires. SEM analysis showed that Ag-nanowires serve as templates in the formation of Ag-ZnO NBs with a one directional shape. The absence of Ag nanowires leads to the radial growth of ZnO with a star-shape morphology. The obtained Ag-ZnO unidirectional structures have potential catalytic, bactericide, conducting applications and also as a nanorotor.

Introduction

Nanorods (NRs), nanotubes, nanowires (NWs) and nanoparticles (NPs) arrays have attracted great interest due to their unique properties and wide range of potential applications in a number of nanotechnologies. The synthesis of metal nanostructures today is one of the most intensively developing fields of preparative chemistry [1-3]. Due to their small sizes and large specific surface areas, nanostructures exhibit novel properties which may significantly differ from those of the bulk materials [4-6]. In particular one-dimensional (1D) nanomaterials have attracted considerable attention for solar cell applications, next-generation field emitters, UV-photodetector, for electronic interfaces with biological systems, gas sensors, catalysis [7-14]. Growth of aligned NRs and NWs is important for applications such as lasers, light-emitting diodes and field effect transistors. ZnO is one of the dominant nanomaterials for development of nanotechnology Recently, a piezo-electric nanogenerator (NG) that converts mechanical energy into electric energy has been developed, based on the coupling of a piezoelectric with the semiconducting properties of ZnO nanostructures [15,16]. Aligned growth of NR's and NW's can be achieved through the use of substrates and catalyst particles or seeds. The large-scale perfect vertical alignment of ZnO nanowires was first demonstrated over a (11 $\bar{2}$ 0) crystal surface of an oriented single-crystal substrate of aluminum oxide (sapphire) [17]. Gold nanoparticles were used as seeds to grow ZnO on a Si wafer [18,19]. In this system the growth is initiated and guided by the Au particle and the epitaxial relationship between ZnO and Si wafer leads to the alignment of the ZnO nanowire [19]. The laterally aligned NWs were prepared by using different materials to activate or inhibit the growth of nanowires [20,21]. In this study, we reported the controlled growth of Ag-ZnO NBs by the precipitation method at room temperature. Ag-NWs were used as precursors to grow the ZnO along this nanostructure. The final shape of this nanostructured material is a brush-like unidirectional structure. This new material can be used as a catalyst for steam reforming or photocatalysis, where silver participates as an active phase [12-14]. However, the Ag-ZnO NBs can also be applied as a conducting material, for bactericidal applications or as a nanorotor.

Experimental

The Ag nanowires were synthesized through a PVP (polyvinylpyrrolidone) assisted reaction in ethylene glycol [22]. An aqueous solution of zinc nitrate ($Zn(NO_3)_2 \cdot 6H_2O$) and the Ag nanowires were mixed under constant stirring, the molar ratio of Ag/ZnO was 0.075. Then, a solution of ammonium hydroxide (NH_4OH) at 28% was added drop wise to complete the precipitation at 19 °C. The solution was stirred for 30 min and the precipitated mixture was aged for 24 h. The residual liquid was removed by decanting. The precipitate was heated at 50 °C for 24 h. The resulting material was then calcined at 500 °C for 5 h under static air, and reduced in H_2 flow at the same temperature for 1h. Finally the sample was cooled down slowly to room temperature (R.T.).

Morphological characterization was performed in a Low Vacuum Scanning Electron Microscope (LVSEM) Jeol JSM-6610-LV at 20 kV, equipped with an Energy Dispersive X-ray Spectroscope (EDX) INCAX-act-Oxford. X-ray diffraction (XRD) powder patterns were recorded in a Siemens D-5000 diffratometer, from 2θ = 27 – 67°, at 40 kV, using Cu Kα (λ = 0.15406 nm), step = 0.026°, time = 3 sec. Rietveld refinement method and TOPAS program were used to determinate the crystallite size and the quantitative phases of the AgNBs from the XRD diffraction patterns. For the TEM and HREM experiments, – the sample weas grinded in an agate mortar and suspended in isopropanol. After ultrasonic dispersion, a droplet was deposited over a carbon coated copper TEM grid. Microstructural analysis was performed in a TEM Jeol JEM 2010, with a resolution of 0.19 nm fitted with an energy dispersive X-ray spectrometer (Noran, model Voyager 4.2.3).

Results and discussion

A typical SEM image of the ZnO structures with a star-shape is shown in Fig. 1a. This sample was prepared without Ag NWs. It can be observed by scanning electron microscopy (SEM), that these structures grow in a radial form with a star-like shape. The peak to peak distance of one of the axis of these ZnO star-shape structures, is

close to 3 μm. In all cases the "cones of the star" were formed by bunches of needles distributed randomly. This kind of morphology was obtained previously on different studies [18,23-25]. In an early study [16] it was suggested that the concentration of [OH⁻] and [Zn²⁺] in the solution, is the most important parameter to obtain these kind of structures, affecting the nucleation and growth of the ZnO structures. A low concentration of [OH⁻] and [Zn²⁺] during the synthesis, prevents the star-shaped structures to grow with a preferential direction in order to obtain unidirectional structures. In this research, Ag nanowires as those in Fig. 1b were used as templates to obtain the Ag-ZnO unidirectional nanostructures. These Ag nanowires have average dimensions of 80 nm in diameter and 15 micrometers in length [22]. The growth direction of the Ag-NWs was along the [1 1 1̄] axis. Analysis of the transversal section of those nanowires was found to have a pentagonal symmetry.

When the Ag NWs and the precursor of the ZnO were added together, the Ag-ZnO NBs-like morphology was obtained, Fig. 1c. It is clear that the Ag-NWs are necessary to obtain the Ag-ZnO nanostructured brush–like morphology, because without them, only individual ZnO nanostars were grown. The energy dispersive spectra of the sample obtained from the SEM-EDS analysis (Fig. 1d) clearly shows that the Ag-ZnO NBs are composed by O, Zn and Ag elements whit an atomic ~ 4:32 Ag:Zn ratio.
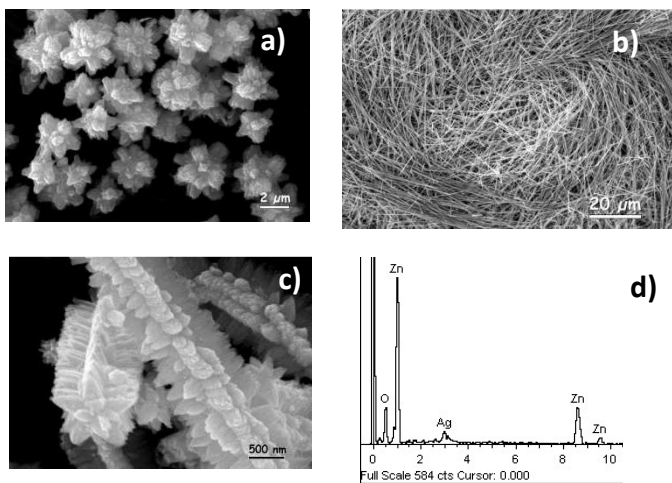

Fig. 1. SEM images of the (a) ZnO structures with a star-shape morphology, (b) Ag nanowires, (c) Ag-ZnO NBs and (d) Energy-Dispersive X-ray spectroscopy of (c) Ag- 4.21 at.%.

Changes on the ZnO morphology due to the introduction of silver into the system was reported by Zhang et al. [26]. They observed that silver influences the growth of the ZnO structures and concluded that it can be used specifically to control the final morphology of the ZnO to achieve a specific type of nanostructure. In our case, we have observed a similar behavior, were the ZnO structures grew along the silver NWs as brushes with a star-like morphology and a five-fold symmetry, Fig. 1c. The distance from cone to cone in the transversal growth axis of these Ag-ZnO unidirectional NBs was close to 1.3 μm, less than that of the star like ZnO structures prepared without silver. Fig. 2 shows the XRD pattern of the ZnO and Ag-ZnO NBs samples after the thermal treatments (calcination and reduction). The X-ray diffraction pattern of the samples was indexed as a hexagonal wurtzite structure of ZnO with lattice parameters a = b = 0.3241 nm and c = 0.5187 nm (JCPDS Card No. 073-8765). These diffraction peaks at scattering angles (2θ) were indexed and indicated in Fig. 2. In addition, diffraction peaks of metallic Ag were present in the Ag-

ZnO NBs samples. No extra peaks related to an intermetallic Ag-Zn compound were observed. These results indicate that the Ag phase remains within the unidirectional structures, even when its original shape is no longer observed. Quantitative phase composition and particle size grain of the Ag-ZnO NBs were determined using Rietveld refinement procedure (SI). The obtained R factors were R_{wp}= 5.393, R_{exp}= 4.846 and χ^2= 1.11. The mean crystallite size of the ZnO of the Ag-ZnO NBs was ca. 8.20 nm. The corresponding quantitative fraction of the Ag and ZnO phases were 10 and 90 wt.% in that order. These values are close to the nominal content in the sample.
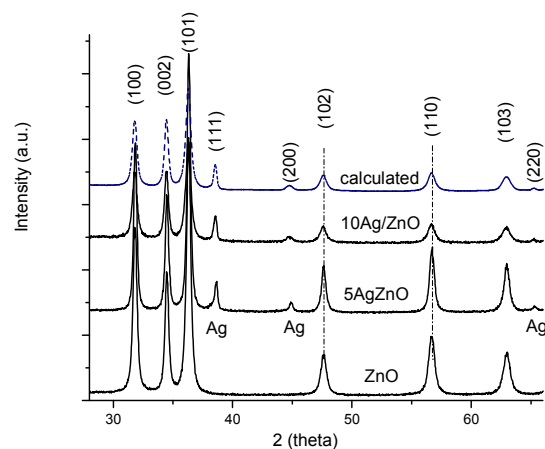

Fig. 2. XRD patterns of ZnO nanostars and Ag-ZnO NBs. The dashed line corresponds to the calculated XRD pattern by Rietveld method.

Typical TEM images of the obtained samples in Figure 3 show the overall morphology of the Ag-ZnO composites. They reveal that this Ag-ZnO NBs grew unidirectionally with a nanostructured brushed-like morphology and cone-like growths on the tips of the structure (Fig. 3a and 3b). EDS analysis of these cones indicated the following elemental composition Zn (60.96 at.%), O (38.43 at.%) and Ag (0.61 at.%) respectively. A transversal view of the Ag-ZnO NBs is presented in Fig. 3c and 3d were the five-fold symmetry is evidenced. It is important to mention that along the unidirectional structure is possible to observe a clear line. This phenomena was observed previously during the preparation of on Ag-CeO₂ nanotubes [13,14]. In which the AgNWs were used to synthesize these kinds of unidirectional structures.

Fig. 4 shows the cross-section images of the Ag-ZnO NBs. were it can be observed that the brushes have a star-like morphology (Fig. 4a and 4b). The width of the star, cone to cone is from 1050 to 1250 nm (Fig. 4c and 4d). In the micrographs of the Ag-ZnO NBs slices, shown in Figure 4a, it can be observed that a few pentagonal Ag-NW can remain in the center of the NBs, which is associated to the highly contrasted structure in the middle of the slice. However, when the Ag NW was removed (clear line in Fig. 3a-b), the presence of a pentagonal central hole, with dimensions between 200 and 350 nm is also evidenced, which might have been caused by the previous existence of the pentagonal NW[22] (Fig. 4b). The arrows in figure 4c and 4d show that the Ag NW is absent in some parts of the Ag-ZnO NBs, which could be the origin of the clear line observed in Fig 3. However, in others zones of the material the Ag NW still remains within the center of the structure. Figure (4c) shows the central black line of 120 nm wide and a grey fringe of approximately 110 nm in

width. According to the EDS analysis, this black line was conformed mainly by silver (76.38 at.%), with a low concentration of Zn (19.74 at.%) and O (3.88 at.%) indicating that the Ag-NW is still present. But, in the grey fringe, Zn (84.83 at.%) and O (13.58 at.%)were the main elements detected along with a small amount of silver (1.59 at.%). According to our observations, we suggest that the Ag-NW might have diffused through the ZnO structure during the thermal treatments following a Kirkendall mechanism. On a first stage, the Ag-NWs were used as templates to grow epitaxially a ZnO phase around the Ag-NW (schema 1). This phenomenon is similar to that reported by Yong Ding et al. [27], where ZnO nanostructures with an asymmetric growth were formed and they named them "combs". In our case, we obtained a well-defined symmetric structure.
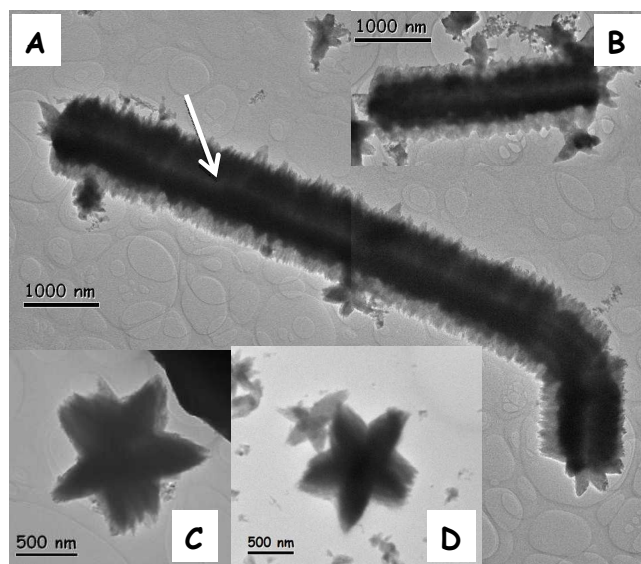

Fig. 3   Ag-ZnO NBs TEM images. a-b) longitudinal view and c-d) transversal view.

Fig. 4 Cross-section TEM images of the Ag-ZnO NBs. Star-like nanostructures (a and b) and Ag-ZnO NBs (c and d).

Figure 4d shows the cross-section image of a Ag-Zn NB where the Ag NW was removed during the synthesis and thermal treatments. The arrow indicates a less contrasted zone of 83 nm in size. It is suggested that this zone was originally occupied by the AgNW. This ZnO structure grew close to 110 nm radially around the Ag-NW, and then continued growing with a star-like morphology which properly formed the brushes. The Ag NW diffused to the ZnO structure through the Kinkerdall effect (schema 1). This effect was observed elsewhere [13,14] in Ag NWs covered by CeO_2, where nanotubes of CeO_2 were grown over Ag NW's and the Ag diffused into the CeO_2 nanotubes during the synthesis process.

A HREM image from the tip of one cone in a Ag-ZnO NBs is shown in Figure 5. In this figure we can observe that the structure is formed by ZnO nanocrystals with an average size of 5 nm. According to the lattice spacing measured, these nanocrystals correspond to a hexagonal phase with parameters a=b= 0.3241 nm and c= 0.5187 nm, previously identified. The inset in figure 5 shows a magnification of one of these nanocrystals, where the incident electron beam is along the [0001] zone axis and the FFT image allowed the identification of the crystallographic planes ($\bar{1}010$) and ($01\bar{1}0$) on it. These ZnO nanocrystals, which grew along the <0002> direction, formed the "bristles". Based on these results it was determined that the brushes grew in that same direction. The dark field image taken with the diffracted (0002) plane of the ZnO, showed that the Ag/ZnO NBs are formed by nanocrystals (SI).
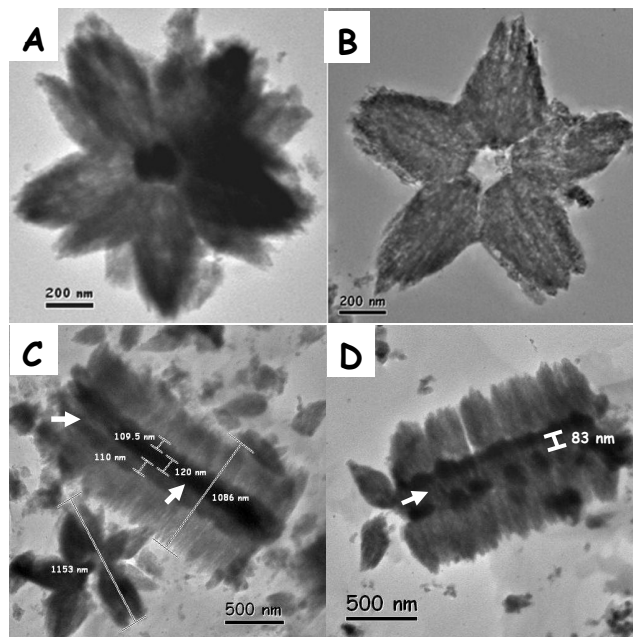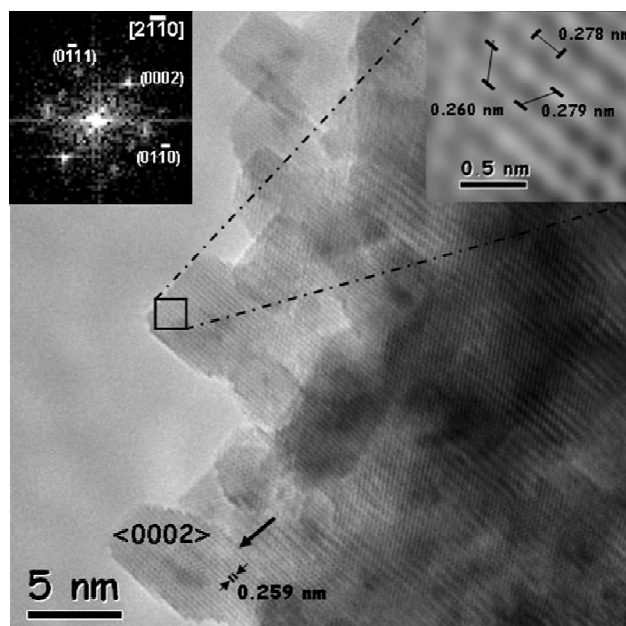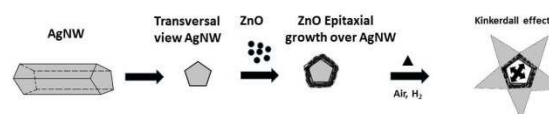

Figure 5 HRTEM image from one of the "cones" shown in figure 4b. Inset shows the FFT and HRTEM of the black frame on the image.

Schema 1. Grow mechanism of the Ag-ZnO NBs

Conclusions

A novel approach to produce unidirectional Ag-ZnO nanostructured brushes has been presented, based on the use of unidimensional AgNW templates. The absence of Ag nanowires leads to the radial growth of ZnO with a star-like shape. For the preparation of the Ag-ZnO NBs, we suggest that in a first stage an epitaxial growth of the ZnO around the Ag-NWs takes place, and then it continues growing until a structure with star-like morphology is obtained, which properly conformed the brushes. During the thermal treatments, the Ag-NW diffuses onto the ZnO structure through a Kirkendall effect and in some of these new NB structures, the Ag-NWs are no longer observed while in others, the Ag-NWs still remain. This could be attributed to a kinetics of the reaction.

Author Information

Corresponding Author

* e-mail address: raul.perez@inin.gob.mx (R. Pérez-Hernández).

Notes

Instituto Nacional de Investigaciones Nucleares, Carr. México-Toluca S/N, La Marquesa, Ocoyoacac, Edo. de México C.P. 52750, México.

References

1. M.C. Daniel and D. Astruc. *Chemical Reviews* 2004, **104**, 293-346.

2. J.C. Love, L.A. Estroff, J.K. Kriebel, R.G. Nuzzo, and G.M. Whitesides. *Chemical Reviews* 2005, **105**, 1103-1170.

3. J. Perez-Juste, I. Pastoriza-Santos, L.M. Liz-Marzan, and P. Mulvaney, *Coordination Chemistry Reviews* 2005, **249**, 1870-1901.

4. S.H. Joo, S. J. Choi, I. Oh, J. Kwak, Z. Liu, O. Terasaki, R. Ryoo*, Nature* 2001, **412**, 169-172.

5. R. Pérez-Hernández, G. Mondragón-Galicia, A. Allende-Maravilla, and J. Palacios. *Physical Chemistry Chemical Physics* 2013, **15**, 12702-12708.

6. T. Trindade, P. O'Brien, and N.L. Pickett, *Chemistry of Materials* 2001, **13**, 3843-3858.

7. L. Zhao, L. Hu and X. Fang. A*dvanced Functional Materials* **22**, 2012, 1551–1566.

8. X. Fang, J. Yan, L. Hu, H. Liu and P. S. Lee. *Advanced Functional Materials*, 2012, **22**, 1613–1622.

9. L. Peng, L. Hu and X. Fang. A*dvanced Materials*. 2013, **25**, 5321–5328.

10. C. M. Lieber. *MRS Bulletin*. 2011, **36**, 1052-1063.

11. G. Xiao, Y. Wang, J. Ning, Y. Wei, B. Liu, W. W. Yu, G. Zou and B. Zou. *RSC Advances*. 2013, **3**, 8104-8130.

12. Z. Li, F. Zhang, A. Meng, C. Xie and J. Xing. *RSC Advances*. 2015, **5**, 612-620.

13. G. Mondragón-Galicia, R. Pérez-Hernández, C.E. Gutiérrez-Wing and D. Mendoza-Anaya. *Physical Chemistry Chemical Physics* 2011, 13, 16756-16761.

14. R. Pérez-Hernándeza, Gutiérrez-Wing, G. Mondragón-Galicia, A. Gutiérrez-Martínez, Francis Leonard Deepak, and D. Mendoza-Anaya. *Catalysis Today* 2013, 212, 225-231.

15. Y. Qin, X.D. Wang, and Z.L.Wang. *Nature* 2008, **451**, 809-813.

16. Z.L. Wang, and J.H. Song, *Science* 2006, **312**, 242-246.

17. M.H. Huang, S. Mao, H. Feick, H. Yan, Y. Wu, H. Kind, E. Weber, R. Russo, and P. Yang*, Science* 2001, **292**, 1897-1899.

18. R. Pérez-Hernández, A. Gutiérrez-Martínez, A. Mayoral, F. Leonard Deepak, Ma. E. Fernández-García, G. Mondragón-Galicia, M. Miki and M. Jose-Yacaman. *Advanced Materials Research* 2010, **132**, 205-219.

19. R. Pérez-Hernández, J.J. Velázquez Salazar, and M. Jose-Yacaman. *Journal Nano Research* 2011, **14,** 69-82.

20. Y. Qin, R.S. Yang, and Z.L. Wang, *Journal of Physical Chemistry C* 2008, **112,** 18734.

21. Z.L. Wang. *Materials Science and Engineering: R:* 2009, **64**, 33.

22. C. Gutiérrez-Wing, C Gutiérrez-Wing, M Pérez-Alvarez, G Mondragón-Galicia, J Arenas-Alatorre, M T Gutiérrez-Wing4, M C Henk, I I Negulescu and K A Rusch*, Journal of Physics: Condensed Matter.* 2009, **21,** 295301.

23. S. Sepulveda-Guzman, B. Reeja-Jayan, E. de la Rosa, A. Torres-Castro, V. Gonzalez-Gonzalez, M. Jose-Yacaman, *Materials Chemistry and Physics* 2009, **115**, 172.

24. L. Feng, L. Feng, J. Liu, J. She, N. Xu, S. Deng, J. Chen. *Journal of Crystal Growth* 2009, **311**, 1435-1440.

25. X. Gao, X. Li, and W. Yu. *Journal of Physical Chemistry B* 2005, **109**, 1155.

26. Y. Zhang and J. Mu. *J. Colloid Interface Sci.* 2007, **309**, 478.

27. Y. Ding, and Z.L. Wang, *Journal of Physical Chemistry B* 2004, **108**, 12280-12291.